

OPTIMISING PERFORMANCE OF SMALL HAWT'S THROUGH IMPROVED ROTOR/ALTERNATOR MATCHING

Mr Kerryn Newey* and Dr Russell Phillips†

*Institute for Advanced Tooling, Walter Sisulu University
knewey@wsu.ac.za

†Department of Mechanical Engineering, Nelson Mandela Metropolitan University
Russell.Phillips@nmmu.ac.za

Centre for Renewable and Sustainable Energy Studies

Abstract

Horizontal Axis Wind Turbines (HAWT's) are the most common and well understood forms of windmills. Typically a large amount of research and development has been invested in the technology of large scale wind turbines. Development of small machines (rotor diameter smaller than 10 m) has not been as forthcoming. Trends in the wind turbine industry have shown that smaller machines tend to be relatively simple devices that have been developed with limited research and development. As a result small turbines can be inefficient, unreliable and expensive to maintain. In many cases rotor design is less than optimal, with very little blade refinement. A significant performance inhibitor is that rotors are typically not well matched to the alternators, thereby reducing performance due to the mismatched systems. The aim of the study is to automate some of the rotor design complexities into a software design tool to improve rotor/alternator matching and therefore small HAWT performance. Blade Element Momentum Theory (BEMT) is used as the mathematical model. A commercially available, Ginlong 1.8 kW Permanent Magnet Generator (PMG), of known performance is used as a benchmark. CFD and experimental testing are used for numerical modelling and validation.

Key words: Small HAWT's; Rotor/Alternator Matching.

1 Introduction

The main purpose of the research is to provide an intuitive spreadsheet based software tool for the optimised design of small horizontal axis wind turbine rotors. The research is targeted at the home builder market as well as smaller commercial manufactures with little or no research and development capacity. It can be seen from Hugh Piggott, (www.scoraigwind.com) a pioneer in the home build wind turbine industry, that this sector is generally large (global) with potential for growth especially in the developing world.

Typically small wind turbines are costly, suffer from poor performance, they tend to be unreliable, are noisy and unsafe. Due to the trend of economy of scale between large machines and the poorly designed small machines, the equivalent performance of small machines is only approximately half that of big machines (Paul Gipe, wind-works.org). A resultant long pay-back period on the initial investment therefore exists and in some cases is never achieved. "Small turbines must become more productive and more reliable to fulfil their promise" says Paul Gipe, wind-works.org. "Home wind turbines are generating a fraction of the energy promised by manufacturers, and in some cases use more electricity than they make, a report warns today", writes Juliette Jowit.

Comments by Michael Klemen on "Simple Rules for Small Wind Turbine Design":

- Make them more user-friendly.
- Make them easier to maintain.
- Make them easier to install.
- Make them cheaper.
- Make them so that nobody notices they are there.

The objective of the research attempts to address some of these issues indirectly through optimisation of performance through improved design.

2 Conceptual Method

In most cases, small wind turbines utilise variable speed direct drive permanent magnet alternators to generate electrical power. The rotor is therefore mounted directly on the alternator drive shaft as a direct coupling. As the wind speed increases, so does the turbine speed and therefore the power output. However, the rotor and alternator performance are governed by fundamentally different equations. Whereas the alternator power (in theory) is essentially a straight line graph (directly proportional to the shaft speed), the rotor power is proportional to the wind speed cubed. The result is the alternator is driven by essentially a “miss-matched” power source.

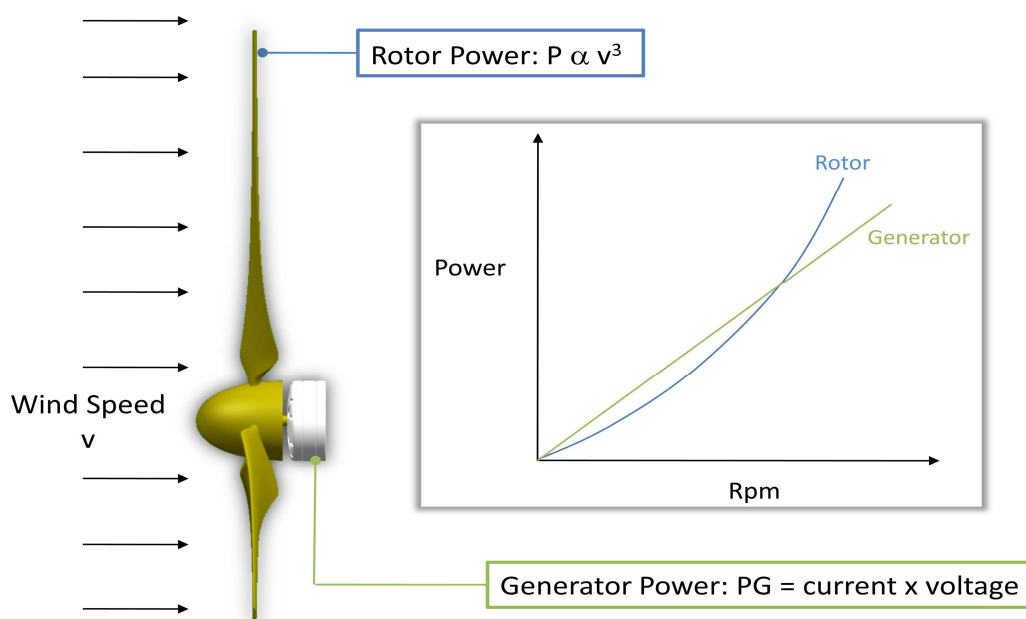


Figure 1. Illustration of theoretical rotor and alternator power curves.

This means that at lower rpm, the alternator can absorb more power than the rotor can produce and at higher rpm (wind speed) the rotor produces more power than the alternator can absorb. The turbine graph is therefore some combination of these two curves. The research does not attempt to address the turbine performance curve, but rather a conceptual method to match the rotor / alternator according to a static “design” or “operating” point; corresponding to the intersection between the two performance curves.

The focus is therefore to develop a spreadsheet design tool based on Blade Element Momentum Theory (BEMT) for rotor design matched to the performance curve of a commercial

(off-the-shelf) permanent magnet alternator. The alternator of choice was the Ginlong GL-PMG-1800, a 1.8 kW 3-phase unit manufactured by Ginlong Technologies, China. Ginlong were able to provide sufficiently detailed performance data for their alternator which made it ideal for the purpose.

The first validation tool used to verify the validity of the spreadsheet design tool is numerical modelling by means of Computational Fluid Dynamics (CFD). The second validation tool is to perform experimental testing.

3 Research Methodology

3.1 BEMT Theory Applied to HAWT Rotor Design

BEMT is considered appropriate design theory for HAWT rotors. The research makes reference from the work done and published by Jansen and Smulders titled "Rotor Design for Horizontal Axis Windmills". The design theory (procedure) is relatively straightforward provided there is a good understanding of some basic ideas and concepts.

The theoretical wind (air) power available in Watts due to the undisturbed wind stream in terms of the rotor cross sectional area is expressed as follows:

$$P_{air} = \frac{1}{2} \rho A V_{\infty}^3 \quad (1)$$

In order to compare characteristics of different wind turbine designs under different wind conditions, mechanical power is multiplied by a factor C_p which is called the power coefficient.

$$P = C_p \frac{1}{2} \rho A V_{\infty}^3 \quad (2)$$

Similarly the local speed u of the rotor at a given radius r divided by the wind speed is termed the local speed ratio.

$$\lambda_r = \frac{u}{V_{\infty}} = \frac{\omega r}{V_{\infty}} \quad (3)$$

More commonly, wind turbines are described by their tip speed ratio (TSR) which is the speed U of the rotor at maximum radius R , divided by the wind speed.

$$\lambda = \frac{U}{V_{\infty}} = \frac{\omega R}{V_{\infty}} \quad (4)$$

The power coefficient C_p in equation (2) is not an efficiency, but may be interpreted as a measure of how successful a wind turbine is in transforming wind energy into mechanical energy. For a specific design of wind turbine, C_p varies with tip-speed ratio. In dimensionless form this is shown in a graphic format of C_p vs λ .

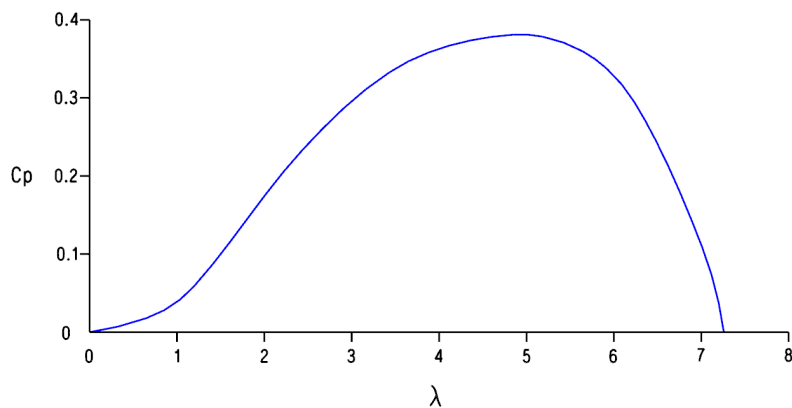


Figure 2. CP vs TSR

This characteristic is independent of air density ρ , wind speed V_∞ and blade radius R . It can also be seen from Figure that an optimum tip speed ratio exists that will give an corresponding maximum value of C_p .

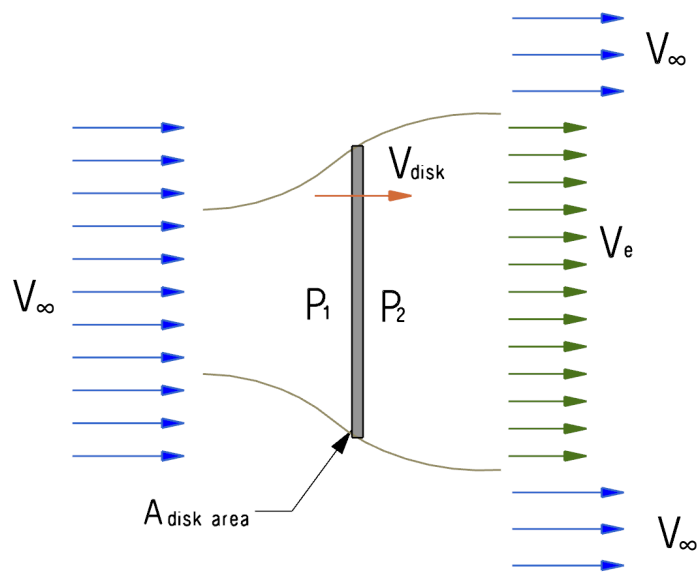


Figure 3. Flow volume for an ideal actuator disk

The power coefficient C_p is defined as a measure of the success a rotor has in extracting mechanical power from the wind. Unfortunately it is not possible to transform all the available kinetic energy into useful power. Assuming the turbine rotor is substituted by an actuator disk, as the wind passes over the disk it decelerates due to the rate of change of momentum. The kinetic energy is therefore reduced and power is extracted. If the free air flow is relatively undisturbed, the mass of air flow will be large but the kinetic energy extracted will be small. Consequently if the kinetic energy extracted is large (i.e. the wind is largely decelerated), the mass flow of air across the disk will be small. Unfortunately not all the kinetic energy can be extracted as the air velocity behind the rotor V_e would be zero! All the air would then be diverted around the rotor and no power would be extracted.

Betz was the first one to show that theoretical maximum energy is extracted if:

$$V_e = \frac{1}{3}V_\infty \quad (5)$$

And;

$$V_{disk} = \frac{2}{3}V_\infty \quad (6)$$

Considering the axial induction factor a (the degree of which the air at the turbine differs from the air far away from the turbine):

$$a = \frac{V_\infty - V_{disk}}{V_\infty} \quad (7)$$

Betz was able to determine an expression for the power coefficient C_p in terms of the axial induction factor a as follows:

$$C_p = 4a(1 - a)^2 \quad (8)$$

Substituting equations (6) and (7) into equation (8) Betz determined the optimum theoretical maximum power coefficient as the Betz limit where;

$$C_p = \frac{16}{27} = 0.593 \quad (9)$$

This value is however only valid for a theoretical design for a high tip speed ratios rotor with an infinite number of blades with zero blade drag and tip losses.

Downstream of the turbine a wake rotation exists due to the tangential component of the velocity over the rotating blades. This wake rotation (opposite in direction to the rotor rotation) constitutes a loss of energy because it contains kinetic energy. For a slowly rotating rotor, the torque is high and the wake rotation losses are high. Conversely a high speed rotor will incur smaller losses. Because the wake loss effect is related to the rotor speed an adjustment can be made to the Betz coefficient in terms of the tip speed ratio λ to approximate the loss as follows:

$$C_{p(wake)} = e^{-0.35\lambda^{-1.29}} \quad (10)$$

The drag coefficient describes the amount of air resistance on the rotating blades. The higher the drag coefficient, the higher the drag force and therefore the losses incurred. The effect on the maximum power coefficient can be described with an approximation in terms of lift vs drag $\frac{C_d}{C_l}$ and tip speed ratio λ as follows:

$$C_{p(drag)} = \frac{16}{27} \cdot \frac{C_d}{C_l} \lambda \quad (11)$$

An approximation to account for losses due to wake rotation, blade drag and tip turbulence on the maximum power coefficient is described in the following equations:

$$C_p = \eta_n [C_{p(ideal)} - C_{p(drag)}] \quad (12)$$

Substituting in for equations (10), (11) and (12) gives:

$$C_p = \left(1 - \frac{1.386}{n} \sin \frac{\phi}{2}\right)^2 \cdot \frac{16}{27} \left(e^{-0.35\lambda^{-1.29}} - \frac{c_d}{c_l} \lambda\right) \quad (13)$$

3.2 Design Point of Operation

The design point (or static point) of operation is defined as the intersection of the rotor and alternator power curves, corresponding to a specific wind speed for the intended operation. The discrepancy in operation between the rotor and alternator means that the rotor and alternator curves can only be made to intersect at one point, the design point of operation. A fast running rotor (high rpm) can be designed to produce the same power as a slow running rotor (low rpm). However, the two rotors will produce different torque corresponding to the power output and this needs to best match the load parameters. When one looks at the alternator load it can be anywhere between these two limits of upper and lower values. It therefore becomes apparent that the performance of the alternator needs to be known so that the rotor can be designed appropriately to “match” the generator. The logical conclusion would be to plot the two curves on a single set of axes corresponding to power output versus rpm, while including the desired wind speed of operation.

The problem becomes progressively more complex when the efficiency of the alternator is considered. Because an alternator is a mechanical device and therefore subject to losses, the rotor has to produce additional power to compensate for this. It is therefore necessary to show both the theoretical and actual alternator performance curves on the same graph to compensate for the losses in the system. The rotor is therefore designed to match the alternator input with the actual turbine output being somewhat smaller.

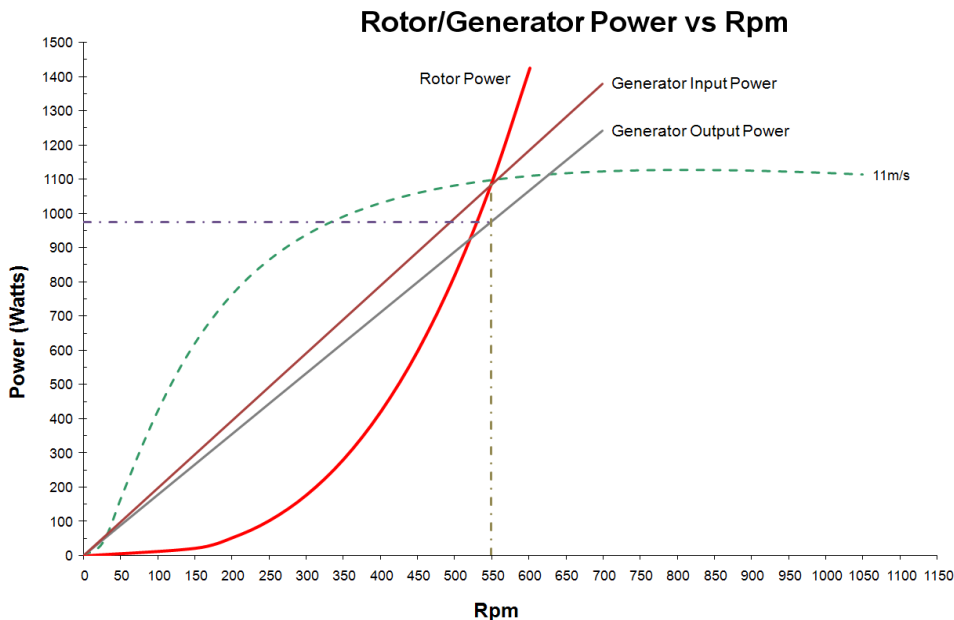


Figure 4. Illustration of the Design Point of Operation including alternator losses

3.3 Rotor Design Tool

The objective of the design tool is to automate the design theory into an Excel spreadsheet. BEMT requires an iterative approach and it is therefore perfectly suited to automated calculations allowing for quicker converge on a suitable design solution. The principle summary of workflow can be split into three sections: Input Parameters, Output Parameters and the Static Operating Point. The variables which most affect the rotor performance are the TSR, the wind speed and the blade radius. As the variables have different effects on the rotor power curve, it can take some time to converge on a solution. The rotor aerodynamic performance is defined by the Reynolds Number of operation. As it is not known at the start of the design, what Re is, a value is assumed, defined as Re critical. The spreadsheet calculates the actual Re corresponding to the design parameter and it is important to check that the Re calculated value is above the (assumed) Re critical value. If Re critical is above the calculated value, the solution is not viable.

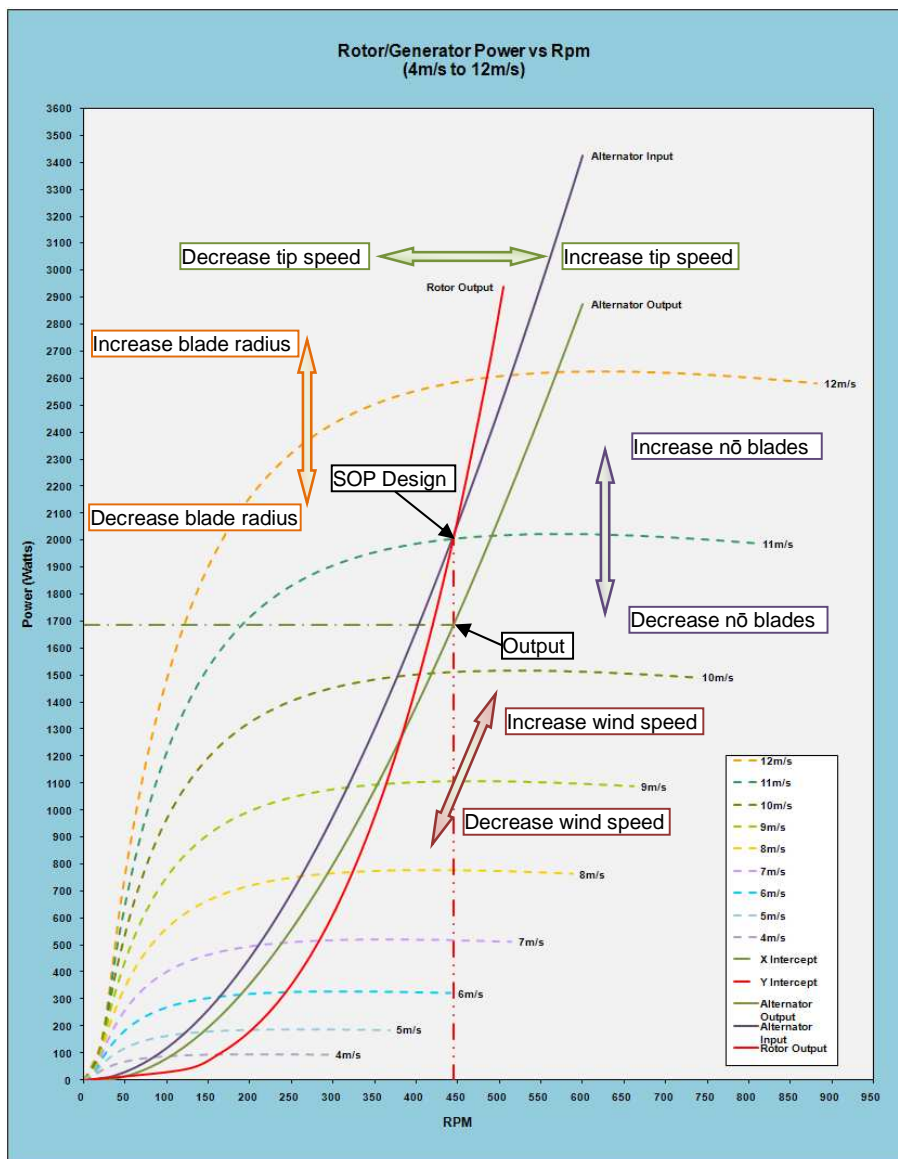


Figure 5. Illustration of the spreadsheet graphical design assistant

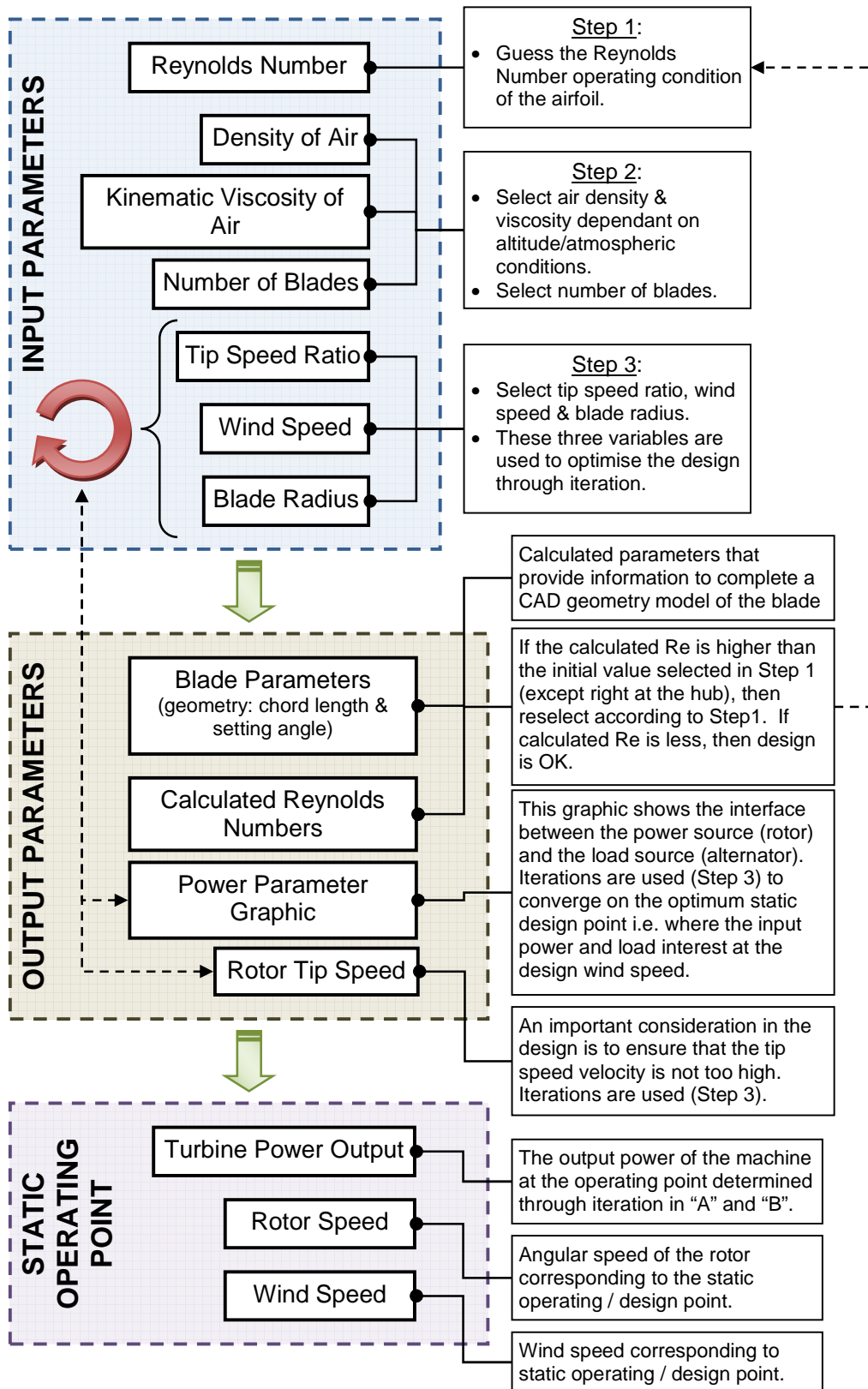


Figure 6. Workflow diagram illustrating the spreadsheet design procedure

4 Results

4.1 Rotor Design and Performance Prediction

Typically there is not necessarily one acceptable result for a particular design due to the combination of variables. The emphasis should be on determining a workable design within the parameters set. In order to validate the spreadsheet design tool, the following rotor design resulted in a workable solution.

Table 1. Alternator specifications, rotor and turbine calculated performance data

Alternator Specifications	
Ginlong Technologies	GL-PMG-1800
Type	Permanent Magnet Generator
Configuration	3-Phase Star Connected AC
Rated Output	1 800 Watts
Rated Speed	489 rpm
Rotor Design Specifications	
Airfoil	NACA 4412
Re Critical	200 000
Re Calculated (lowest)	229 900
Angle of Attack	6
Lift Coefficient	1.017
Drag Coefficient	0.016
Centre of Pressure	35% of chord
Air Density	1.225 kg/m ³
Air Kinematic Viscosity	1.5 E-5 m ² /s
Number of Blades	3
Tip Speed Ratio	5.5
Rated Wind Speed	11 m/s
Blade Radius	1.3 m
Rotor Power Output	2 003.45 Watts
Rotor Speed	444.41 rpm (46.54 rad/s)
Rotor Torque	43.05 Nm
Turbine Theoretical Performance Prediction	
Rated Power Output	1 685 Watts
Rotor speed	444 rpm
Rated Wind Speed	11 m/s
Rotor Loading	377 W/m ²

4.2 Blade CAD

The blade was modelled as a 3D solid model in Siemens NX using the NACA 4412 polar plots extracted from VisualFoil software. 22 Sections were used with ideal taper and twist from the blade root to the tip. The airfoil profiles were aligned axially with their respective centres of pressure to eliminate any adverse twisting due to off-axis aerodynamic loading.



Figure 7. Blade designed in Siemens NX CAD software

4.3 Numerical Modelling in FloEFD

The purpose of CFD numerical modelling was to verify the validity of the spreadsheet design tool and therefore the blade design (Table 1). FloEFD, by Mentor Graphics, a concurrent engineering based CFD software was chosen for the simulation. As the point of interest is the singular “Design Point of Operation”, the CFD model is non-transient and therefore significantly simplified. The rotor was modelled fully in 3D utilising the exact blade CAD geometry featuring a sharp trailing edge. A fluid velocity of 11 m/s corresponding to the air flow was applied to the rotor. The rotation of the rotor was simulated by a rotating region with an angular velocity of 46.54 rad/s. The analysis was set to external with flow criteria were laminar and turbulent. The turbulence parameters were set at 100% over 6.5 m. A sufficiently large rectangular computational domain was chosen to allow for fully developed flow (Hartwanger and Horvat, 2008).

Table 2. Illustration of Computational Domain size as a factor of rotor diameter

Computational Domain		
X	+2.5 m	0.96 x Rotor Diameter
	-2.5 m	
Y	+2.5 m	0.96 x Rotor Diameter
	-6.5 m	2.50 x Rotor Diameter
Z	+2.5m	0.96 x Rotor Diameter
	-2.5 m	

FloEFD is a CFD tool for engineering type applications featuring robust and efficient built in automatic computational meshing tools. However, a manual mesh method was chosen over the automatic mesh settings to achieve a sufficiently dense mesh in the computational domain. The mesh is more refined (dense) in the immediate vicinity of the rotor with a gradual expansion factor applied outwards towards the mesh boundary. The result is a mesh which is significantly refined for the analysis and the optimisation of solver recourses.

Table 3. Number of cells and distribution related to the computational mesh

Mesh Statistics (Number of Cells)	
Total Cells	4 1 22 038
Fluid Cells	2 498 709
Solid Cells	614 983
Partial Cells	1 008 346

A significantly more refined (denser) mesh was applied to the local rotating region solid volume. This was necessary to accurately predict the flow conditions over the blade airfoil profiles

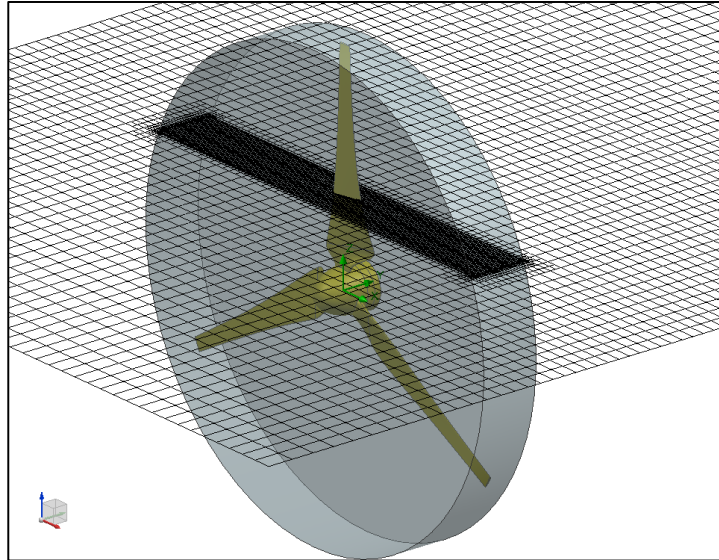


Figure 8. A cutplot showing the high mesh refinement applied to the rotating region

A Torque (Y) global goal was set for the convergence criteria. A mesh independent solution was obtained after 321 iterations and a CPU time of 79 192 s. The solution for rotor torque was 38.93 Nm which was within 10% of the theoretical values determined by the spreadsheet.

4.4 Blade Laminate Design and Manufacturing

The laminate design was modelled in Patran/Nastran with reference to the Fibre Glass Wind Turbine Manufacturing Guide (Corbyn and Little). The layup was designed to optimise blade stiffness through a combination of carbon (predominantly) and glass fibre reinforcement featuring a central spar to further enhance bending stiffness.

Table 4. Laminate material values

Material	Glass content (mass)	Density (kg/m ³)	Elastic Modulus E (GPa) 0°	Shear Modulus G (GPa)	Poisson's Ratio (Ea/Eh*Vh/a)
Carbon UD	50%	1650	94.83	3.01	0.32
Carbon 0/90	50%	1650	42.40	5.10	0.05
Glass UD	50%	1650	32.30	3.13	0.30
Glass Biaxial	50%	1650	17.80	3.26	0.05

Table 5. Laminate material values

Material	Ultimate Tensile Strength (MPa) 0°	Ultimate Compressive Strength (MPa) 0°	In-Plane Shear Stress (MPa)
Carbon UD	946.80	520.74	44.31
Carbon 0/90	418.86	258.54	51.56
Glass UD	615.73	355.00	50.00

Glass Biaxial	277.00	162.00	86.00
---------------	--------	--------	-------

Table 6. Laminate layer thickness

Layer	Layer Thickness
1 layer 200g/m2 Carbon or Glass	0.2 mm
1 layer 400g/m2 Carbon or Glass	0.4 mm

The blades were manufactured in a two-part mould machined on a CNC router from polyurethane tooling board. The leading and trailing blade surfaces were moulded separately by means of vacuum infusion and bonded together after curing. A joggle was included to increase bonding surface area to ensure a strong joint. Finally the blades were painted using a polyurethane 2K automotive paint finish as protection for the non UV stabilised Mpreg 22 epoxy resin.

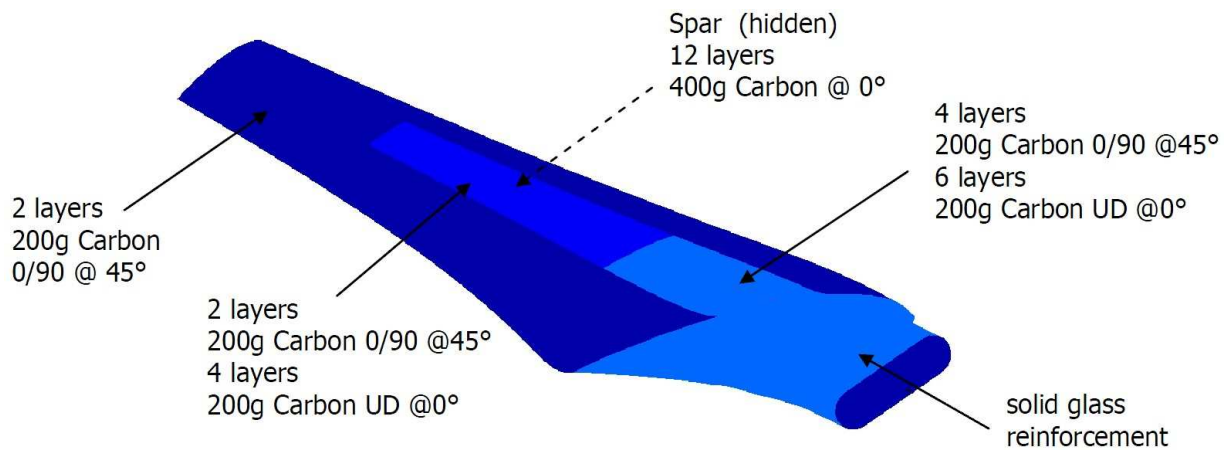


Figure 9. Blade laminate layup

The laminate design and manufacturing was outsourced to the Technology Station based Durban University of Technology. The laminate modelling conducted by Mr Ryan Hamilton and the manufacturing of the moulds and blades was completed in their workshop under the management of Mr Ebrahim Cassim.

4.5 Experimental Validation

The experimental validation proposes a test of the assembled turbine in a free air controlled velocity stream (Larwood, Scencenbauch and Acker, 2001). A lattice framework has been manufactured for mounting the turbine onto the back of a light delivery vehicle. Three important data require measurement: wind speed, turbine shaft speed and output from the turbine. The experiment has been set up in such a way to measure power output directly from the 3-phase star-connected AC generator output, wired directly to the load bank. The load bank is configured as a resistor load bank consisting of three resistors, star-connected AC. The data logging system is supplied by Campbell Scientific SA, including an RM Young Wind Sentry set and a hall effect zero speed sensor supplied by the Magnetic Sensors Corporation. Initially it was planned to measure the generator power output directly by means of a Wattnode Modbus, configured to the data logger. This proved not to be a viable measurement option. The challenge is to measure fluctuating phase voltage, with fluctuating current and variable frequency. An alternative solution is being investigated that will make use of potential voltage and current transformers from Magnelab to replace the Wattnode Modbus setup.

5 Conclusions and Recommendations

Automation of the BEMT theory as presented by Jansen and Smulders into a comprehensive Excel spreadsheet substantially decreases the iteration time required for rotor design. Various theoretical blade options can be configured quickly and intuitively compared to performance criteria. Although the research was based only on Naca 4412 airfoil data and a Ginlong GL-1800-PMG alternator, any number of airfoil and alternators (of known performance) can easily be incorporated.

Full 3D numeric modelling in FloEFD provided a reasonably good match to the theoretical values. FloEFD tended to under-predict the rotor performance compared to the theoretical values. The result was obtained with the highest mesh density possible that the server could solve. To date the experimental validation has not been concluded, and therefore a definitive conclusion cannot be drawn as to the prediction accuracy of the design tool and indeed the CFD. However, the solution is within reasonable calibration limits.

The initial objective of the spreadsheet design tool was to provide manufacturers of small HAWT's with a tool to improve rotor designs with a resultant improvement in turbine performance. The reality is that without a very good understanding of rotor design and small HAWT operation, the design tool has limited value. However, with skilled use, it has potential for substantial validity. With a more robust theory incorporated into the spreadsheet (especially considering blades with multiple airfoil profiles) it can potentially have a much larger and significant impact as a useful design tool for large scale turbines.

The results from the initial scope of work support the theoretical design data and the validation methodology based on CFD analysis. Further experimental validation and calibration to correlate the design tool offers a potentially economical methodology for improving windmill design.

References

Piggott, Hugh. www.scoraiqwind.com.

Gipe, Paul. www.wind-works.org/SmallTurbines/Gipe%20CLER%20Paris%202010-05-07.pdf.

Jowit, Juliet, 13 January 2009, *Many Home Turbines Fall Short of Claims, Warns Study*. The Guardian.

Klemen, Michael. www.wind-works.org/articles/simplerules.html

Jansen, W.A.M. and Smulders, P.T., May 1977, *Rotor Design for Horizontal Axis Windmills*. Publication SWD 77-1

Hartwanger, David and Horvat, Dr Andrej, 2008, *3D Modelling of a Wind Turbine Using CFD*. NAFEMS Conference, United Kingdom.

Corbyn, Andrew and Little, Matthew, May 2008, *Fibre glass wind turbine blade manufacturing guide*. Engineers Without Borders (EWB – UK) & Sibol ng Agham at Teknolohiya (SIBAT – Philippines).

Larwood, Scott, Sencenbaugh, Jim and Acker, Brian, June 2001 *Controlled Velocity Testing of an 8-kW Wind Turbine*. NREL, Presented at the American Wind Energy Association's WindPower Conference, Washington, D.C.

ERROR: syntaxerror
OFFENDING COMMAND: --nostringval--

STACK:

/Title
()
/Subject
(D:20121113085750+02'00')
/ModDate
()
/Keywords
(PDFCreator Version 0.9.5)
/Creator
(D:20121113085750+02'00')
/CreationDate
(jhl2)
/Author
-mark-